Published in final edited form as:
Nat Genet. 2013 March ; 45(3): . doi:10.1038/ng.2533.

The nexin-dynein regulatory complex subunit DRC 1 is essential for motile cilia function in algae and humans

Maureen Wirschell[1,#,10], **Heike Olbrich**[2,#], **Claudius Werner**[2], **Douglas Tritschler**[3], **Raqual Bower**[3], **Winfield Sale**[1], **Niki T. Loges**[2], **Petra Pennekamp**[2], **Sven Lindberg**[4], **Unne Stenram**[4], **Birgitta Carlén**[4], **Elisabeth Horak**[5], **Gabriele Köhler**[6], **Peter Nürnberg**[7,8,9], **Gudrun Nürnberg**[7,8,9], **Mary E. Porter**[3,*], and **Heymut Omran**[2,*]

[1]Department of Cell Biology Atlanta, Emory University School of Medicine, GA, USA

[2]Department of Pediatrics, University Hospital Muenster; Germany

[3]University of Minnesota, Minneapolis, MN, USA

[4]Department of Otorhinolaryngology – Head and Neck Surgery, Lund University and Skane University Hospital (SUS) Lund, Sweden

[5]Department of Pediatrics and Adolescents, Division of Cardiology and Pulmonology, Innsbruck Medical University, Austria

[6]Institute of Pathology, University Hospital Muenster; Germany

[7]Cologne Center for Genomics, University of Cologne, Cologne, Germany

[8]Center for Molecular Medicine Cologne (CMMC), University of Cologne, Cologne, Germany

[9]Cologne Excellence Cluster on Cellular Stress Responses in Aging-Associated Diseases (CECAD), University of Cologne, Cologne, Germany

Corresponding addresses: Heymut Omran; Department of Pediatrics; University Hospital Muenster; Albert Schweitzer Campus 1; 48149 Muenster, Germany. heymut.omran@ukmuenster.de; Mary Porter; Department of Genetics, Cell Biology, and Development, 6-160 Jackson Hall, University of Minnesota, 321 Church St. SE, Minneapolis, MN 55455, USA. porte001@umn.edu.
[10]Current address: Department of Biochemistry, University of Mississippi Medical Center, Jackson, MS, USA.
[#]Authors contributed equally to the work.
[*]Authors jointly supervised the work.

URLs.
Chlamydomonas genome database (JGI version 2.0; http://genome.jgi-psf.org/Chlre2/Chlre2.home.html).
Volvox genome Database (http://genome.jgi-psf.org/Volca1/Volca1.home.html).
Center for Mass Spectrometry and Proteomics (University of Minnesota http://www.cbs.umn.edu/msp/).
Support of the Center for Mass Spectrometry and Proteomics at the University of Minnesota is described at http://www.cbs.umn.edu/msp/about

Contributions
D.T. and M.W. cloned the *DRC1* gene and generated the antibody against DRC1. D.T. identified the *pf3* mutation. R.B. performed biochemical studies on *Chlamydomonas* axonemes. M.E.P. evaluated the spectral counting and *pf3* mapping data. H. Olbrich evaluated linkage analysis and performed sequencing of PCD patients. C.W. evaluated clinical data from PCD individuals and performed high-speed videomicroscopy analysis and nasal NO of OP-26II1. N.T.L. performed high-resolution immunofluorescence microscopy (IF) of PCD samples. P.P. generated *in situ* hybridization of Ccdc164 at the mouse embryonic node and performed IF. H. Olbrich, N.T.L., P.P., D.T., R.B., and M.W. prepared figures. S.L., U.S. and B.C. provided clinical data, TEM and DNA of OP-39 and OP-56. E.H. provided clinical data and DNA of OP-26. G.K. performed TEM. P.N. and G.N. performed linkage and haplotype analyses. H. Omran evaluated all TEM analyses. H. Omran, W.S., and M.E.P. coordinated the study. M.W., M.E.P, nd H. Omran wrote the manuscript.

Author information: *Chlamydomonas* DRC1 sequences have been deposited into GenBank with the following accession numbers: *Chlamydomonas* DRC1 cDNA; JX311620; *Chlamydomonas* DRC1 protein; accession # AFU81554. The Human DRC1 protein (also known as C2orf39 and CCDC164) is NP_659475.2. Reprints and permissions information is available at www.nature.com/reprints. The authors claim no competing financial interests.

Summary

Primary ciliary dyskinesia (PCD) is characterized by dysfunction in respiratory and reproductive cilia/flagella and random determination of visceral asymmetry. Here, we identify the DRC1 subunit of the Nexin-Dynein Regulatory Complex (N-DRC), an axonemal structure critical for regulation of the dynein motors, and demonstrate that *DRC1/CCDC164* mutations are involved in the pathogenesis of PCD. Loss-of-function *DRC1/CCDC164* mutations result in severe defects in assembly of the N-DRC structure and defective ciliary movement in *Chlamydomonas* and humans. Our results highlight the role of N-DRC integrity for regulation of ciliary beating and provide the first direct evidence that *drc* mutations cause human disease.

Keywords

cilia; dynein; primary ciliary dyskinesia (PCD); Nexin-Dynein Regulatory Complex (N-DRC)

Defects in ciliary assembly and function are responsible for a wide-range of human diseases and syndromes called the “ciliopathies” including primary ciliary dyskinesia (PCD), which is a genetically heterogeneous group of recessive disorders characterized by defects in ciliary motility[1]. PCD patients suffer from chronic destructive airway disease caused by abnormal muco-ciliary clearance of the airways. Abnormal sperm flagella propulsion contributes to male infertility. In most PCD variants, randomization of left-right body asymmetry is observed due to defective nodal cilia motility, and approximately half show *situs inversus* or *situs ambiguous*[2]. PCD mutations have been identified in genes encoding subunits (*DNAH5*, *DNAH11*, *DNAI1*, *DNAI2*, *TXNDC3*, *DNAL1*) or assembly factors (*KTU*, *LRRC50*) of dynein arms[2–4]. In addition, mutations have been reported in genes encoding components of the radial spokes (*RSPH4A*, *RSPH9*) that result in an intermittent or complete loss of the central apparatus microtubules, and CCDC103, which uniquely localizes to both the cytoplasm and the axoneme[5].

Ciliary structures important for regulation of the dynein motors include the central pair apparatus, the radial spokes and the nexin link-dynein regulatory complex (N-DRC)[6–9]. Very recently, we reported that mutations in *CCDC39* and *CCDC40* cause a novel PCD variant characterized by altered ciliary beating due to defects in the assembly of both the N-DRC and inner dynein arms[10,11]. However, given the broad range of structural defects observed in these patients[12], it is unclear if these proteins are components of the N-DRC or another axoneme sub-structure. The N-DRC is a large, complex structure that is anchored to the A-tubule of the outer doublet near radial spoke S2 and extends towards the B-tubule of the adjacent outer doublet—resulting in a link that connects the outer doublets[13]. The N-DRC is ideally positioned to transmit signals from the central pair and radial spokes to the inner and outer dynein arms; however, the mechanism of how the N-DRC regulates dynein function is unclear.

In genetic screens to identify suppressors of paralyzed flagellar mutants in the green alga *Chlamydomonas*[7], several mutants (termed *drc* mutants) were identified that disrupt the N-DRC structure and closely associated inner dynein arms[8,9,13,14]. Structural and biochemical analysis of *drc* mutants indicates that the *Chlamydomonas pf3* mutant is defective in DRC1 and manifests the most severe defect in inner dynein arm and N-DRC assembly of all of the *drc* mutants[8,9,13,14]. Like other *drc* mutants, *pf3* cells display reduced swimming speed and abnormal ciliary waveform characterized by reduced shear amplitude[15].

Of the known DRC components, only *DRC4* (human orthologue *GAS8;* also known as *GAS11*) and *CMF70* in *Trypanosoma brucei* (orthologue of DRC2 in *Chlamydomonas*) have been cloned and characterized at the molecular level as *drc* mutations[16,17]. A

requirement for GAS8/GAS11 in ciliary motility and vertebrate development has been recently demonstrated in zebrafish: *gas8* morphants exhibit several developmental defects typical for ciliary morphants and mutants including hydrocephaly, neural cell death, left-right axis defects, and impaired otolith biogenesis[18]. Several candidate DRC subunits have been identified by comparative 2D gel-based proteomics, with the exception of DRC1 (Supplementary Table 1)[19]. Here, we identify a novel gene encoding the DRC1 component in *Chlamydomonas* and further demonstrate that the integrity of the N-DRC is essential for the regulation of ciliary beat and that loss of the N-DRC results in primary ciliary dyskinesia in humans.

Results

Identification of the *Chlamydomonas* DRC1 subunit

To identify the *Chlamydomonas* DRC1 subunit, we obtained the sequence of two DRC1 peptides, YLAAVEAYQSQLEG and QFVEVQNAYKE (courtesy of Gianni Piperno, Mount Sinai School of Medicine), by direct amino acid sequencing of protein obtained from 2D gels of wild-type axonemes (see Methods). The two peptides were used to search the *Chlamydomonas* genome database (JGI version 2). Peptide YLAAVEAYQSQLEG detected an unplaced genomic read (TIN310364.b1) while the other peptide yielded no hits in the database. Using the small amount of genomic sequence from TIN310364.b1, we analyzed *Volvox* genomic sequences and identified several overlapping sequences that were compiled into a consensus sequence and used to blast the NCBI database. A candidate human protein was identified (NP_659475.2 also called C2orf39 or CCDC164) and used to re-screen the *Chlamydomonas* genome database. This approach detected several unplaced genomic reads in the 5′ and 3′ end of the gene. Using PCR-based methods, we obtained the sequence of the full-length *DRC1* cDNA (Supplementary Table 2, Supplementary Fig. 1a). Southern and Northern blot analyses indicate that *DRC1* is a single copy gene and its mRNA is upregulated by deflagellation—a hallmark feature of mRNAs that encode ciliary proteins in *Chlamydomonas*[20] (Supplementary Figs. 1b and c). As expected, the cloned sequences map to the *PF3* locus (Supplementary Table 3, Supplementary Figs. 1d and e). The ORF predicts a highly conserved, coiled-coil protein of 698 amino acids with a mass of 79.3 kDa and a predicted pI of 5.57 (Fig. 1), values consistent with those previously published for DRC1[8]. The DRC1 subunit has orthologues in organisms with motile cilia including the predicted human protein CCDC164 (Fig. 1 and Supplementary Fig. 2).

Characterization of the *Chlamydomonas* mutant *pf3*

To confirm that DRC1 is defective in *pf3*, we sequenced the *DRC1* gene in *pf3* and discovered a mutation that converts Serine 6 to a stop codon (Fig. 1 and Supplementary Fig. 3). The mutation predicts that the *pf3* mutant will express no DRC1 protein and is effectively a null allele. Consistent with this prediction, no DRC1 protein is detected in *pf3* axonemes (Fig. 2a) using an antibody specific for the DRC1 protein (Supplementary Fig. 4). The band detected by the DRC1-specific antibody migrates on SDS-PAGE with a Mr of ~80 kDa, consistent with the predicted mass for DRC1. Also consistent with previous reports[8,9,19], DRC1 is present in the *drc* mutants *pf2*, *sup-pf4* (*drc5*) and *sup-pf3* (*drc4*), as well as in mutants missing the outer dynein arm (*pf28* and *sup-pf2*), the inner arm I1 or dynein *f* (*pf9*), and inner arm dyneins *a, c* and *d* (*ida4*) (Fig. 2a).

To determine if DRC1 is a *bona fide* subunit of the N-DRC, we analyzed ciliary fractions for the presence of the DRC1 protein (Fig. 2b). DRC1 is present in isolated axonemes and is not readily extracted by high salt buffers that typically remove the dynein arms (0.6 M NaCl). DRC1 is released from the outer doublet microtubules with other DRC subunits by extraction with sodium iodide, conditions previously reported to release the radial spokes[8].

In contrast, the DRC subunits that remain in *pf2* and *pf3* axonemes are more readily extracted than the DRC subunits in wild-type axonemes. DRC1, present in *pf2* axonemes, and DRC4, present in reduced amounts in *pf3* axonemes, are readily extracted by 0.6 M NaCl, indicating that the association of the N-DRC with the outer doublet microtubules is compromised in these mutants.

Furthermore, DRC1 sediments with DRC4 as part of a large complex that is greater than 19S (Fig. 2c) in sucrose gradients of NaI extracts from a representative wild-type strain (*pf2:PF2-HA*) expressing an HA-tagged DRC4 subunit[17]. RSP16, a subunit of the radial spokes, and CaM-IP3 (FAP61), a subunit of the CSC, also co-sediment at ~19S, but the peak of these two proteins is shifted slightly relative to the peak fractions of the DRC subunits (Fig. 2c). Interestingly, sedimentation of the N-DRC complex is altered in extracts from the *drc* mutant *pf2*, where DRC1 sediments more broadly throughout the gradient, with a small peak at ~19S. In *pf3* extracts, DRC4 sediments at ~2S (Fig. 2c) indicating that the DRC subunits that remain in *pf3*, dissociate into smaller sub-complexes.

Previous biochemical and structural analyses have demonstrated that *pf3* is severely defective in assembly of the N-DRC and several inner arm structures[8,9,13,14]. Further biochemical analysis of the *pf3* mutant confirms that DRC1 is required for the efficient assembly of certain inner dynein arm subunits as well as subunits of the Calmodulin-Spoke associated Complex (CSC)[19,21]. It was previously reported that a spot on 2D gels containing both the IC140 subunit of inner arm I1 and the FAP61 (CaM-IP3) subunit of the CSC was reduced in *drc*-mutant axonemes[19]. Here we show directly by Western blot with specific antibodies that assembly of FAP61 (CaM-IP3) is reduced in *pf3* axonemes (Fig. 2d), whereas IC140 levels are unaffected. These observations are consistent with recent findings that the CSC is located at the junction of radial spoke S2 and the N-DRC[21]. Antibodies directed against the radial spoke subunit, RSP16, and a conserved CCDC39 peptide indicate that the levels of these two proteins are not significantly altered in *pf3* axonemes (Fig. 2d), consistent with previous reports[19]. However, consistent with earlier studies[22], tektin antibodies indicate that tektin is significantly reduced in *pf3*.

Previous SDS-PAGE analyses have indicated that inner arm DHC bands are reduced ~50% in *pf3* axonemes, and analysis of dynein extracts by FPLC has demonstrated a specific deficiency in inner arm dynein *e* corresponding to DHC8[8,14,23]. Structural analysis by cryo-ET has revealed that at least two inner arm densities are defective in *pf3* axonemes; one density by radial spoke S2, corresponding to dynein *e*, and one density distal to S2, corresponding to either dynein *b* or dynein *g*[13]. More recently, cryo-ET of *Chlamydomonas* axonemes has resolved the positions of several inner arm dyneins in the 96 nm axoneme repeat, and these authors proposed that dynein *g* is located at the position just distal to radial spoke S2[24].

To more clearly define the specific inner arm defects in *pf3*, we assessed the levels of several inner arm subunits in *pf3* relative to wild type. Western blots probed with antibodies for DHC5 (dynein *b*), DHC9 (dynein *c*) and DHC11 do not detect major reductions in these DHC isoforms (Fig. 2d). DHC11, as well as DHC3 and DHC4, are heavy chain subunits of uncharacterized inner arm dyneins that are located in the proximal region of the axoneme[23]. The levels of Rib72, an integral component of the outer doublet microtubules, are also unchanged in *pf3* mutant axonemes. However, the light chain subunits associated with inner arm dynein *d* (p44, p38 and p28), inner arm dynein *a, c*, and *d* (p28) and inner arm dyneins *b, e*, and *g* (centrin) are all reduced in *pf3* axonemes, indicating that the assembly of multiple inner arm isoforms is affected by loss of DRC1.

To further assess the inner arm defects in *pf3*, we analyzed the DHC content of wild-type and *pf3* axonemes by mass spectrometry and spectral counting (Supplementary Fig. 5). The total number of assigned spectra for each DHC was compared to the total number of assigned spectra for the two DHCs of the I1 dynein. Analysis of total spectra indicates reductions in DHC2 (dynein *d*), DHC4 (minor inner arm species), DHC7 (dynein *g*) and DHC9 (dynein *c*), and the complete absence of DHC8 (dynein *e*). The absence of DHC8 (dynein *e*) and the significant reduction in DHC7 (dynein *g*) are consistent with the cryo-ET studies described above[13,24]. The observed reductions in DHC2 (dynein *d*) and DHC9 (dynein *c*) have not yet been correlated with structural defects, but it is interesting to note that both of these dyneins are located in the distal half of the 96 nm axoneme repeat. DHC3 (minor inner arm species), DHC6 (dynein *a*) and DHC11 (minor inner arm species) are not significantly changed in *pf3* while the abundance of DHC5 appears slightly increased by this method. Thus, mutations in the DRC1 subunit result in profound defects in the assembly of specific inner arm DHCs (Supplementary Fig. 5), and all of the affected DHCs have been localized in close proximity to the N-DRC by independent structural studies[8,9,13,14].

The Human DRC1 orthologue is mutated in PCD patients

Based on the well-characterized ciliary phenotype of the *Chlamydomonas pf3* mutant, we considered the human *DRC1* orthologue, *CCDC164*, to be a prime candidate for PCD. Notably, the *CCDC164* gene is primarily expressed in lung, brain and prostate[25]. We performed total genome scans by using single-nucleotide polymorphism (SNP) arrays (10K Affymetrix SNP array; Affymetrix, Santa Clara, CA USA) in several PCD families (data not shown). In the PCD family OP-26, linkage analysis identified a positional candidate-gene region on chromosome 2 (13 Mb, Zm-1.20) that contains the *CCDC164* gene. Haplotype analysis was consistent with homozygosity by descent (Supplementary Fig. 6). Amplification and sequencing of the *CCDC164* exons identified a homozygous nonsense mutation (c.2056A>T) which predicts a premature stop of translation (p.Lys686*) in patient OP-26II1; both parents were heterozygous carriers of the mutation (Supplementary Fig. 3b). OP-26II1 is a 15-year old Austrian male of Turkish ancestry. The parents are not consciously consanguineous but originate from the same remote region. He has suffered from neonatal respiratory distress, recurrent pneumonia since infancy, chronic suppurative otitis media and chronic sinusitis, findings typically observed in PCD. Computed tomography, performed at the age of 12 years, revealed bronchiectasis particularly of the middle lobe together with mucus plugging (Supplementary Fig. 3c). Other diseases, notably cystic fibrosis were excluded by extensive investigations. Nasal nitric oxide (NO) measurement revealed a markedly reduced nasal NO production rate of 14,6 nl/min consistent with the diagnosis of PCD[26].

To investigate the structural defects in *CCDC164* (*DRC1*)-defective human cilia, we examined axonemal structure by transmission electron microscopy (TEM) and high-resolution immunofluorescence (IF) microscopy. Respiratory cilia have a characteristic 9+2 arrangement of ciliary microtubules, along with axonemal structures like the radial spokes, dynein arms and the N-DRC (Fig. 3a and b). Normal ciliary 9+2 organization and N-DRC structure (Fig. 3a) is diagramed for clarity. The region around the N-DRC is enlarged to show the predicted locations of DRC subunits within the N-DRC structure. Interestingly, most cross-sections of nasal respiratory cilia from OP-26II1 exhibited no dramatic alterations in the arrangement of outer doublet microtubules (Fig. 3b,c). Only a few cilia showed unspecific ultrastructural alterations including substitution of peripheral doublets by single tubules or presence of super-nummary single tubules. However, careful analysis of the cross-sections identified more subtle ultrastructural changes indicative of alterations in the N-DRCs. In normal patients, some nexin links can be visualized per cross-section in almost every cilium by routine TEM[27]. Notably, in *CCDC164* mutant respiratory cilia we

did not observe any nexin links in all of the analyzed cross-sections, consistent with structural analyses of *pf3* by image averaging of TEM sections and cryo-electron tomography[13,14]. Our ultrastructural findings resembled reported observations in two Swedish families (OP-59; OP-39) with three affected PCD individuals possibly caused by absence of nexin links[27]. Respiratory cilia from one of these PCD individuals (OP-59II2) show normal 9+2 ciliary microtubule organization with an absence of any observable N-DRC links (Fig. 3d).

Ultrastructure of the outer and inner dynein arm structures appears normal, which we confirmed by IF using antibodies specific for the outer arm (DNAH5) and inner arm (DNALI1-orthologous to *Chlamydomonas* p28 light chain) dynein subunits (Supplementary Fig. 7). Notably, a p28 reduction was observed in *Chlamydomoans pf3* axonemes, whereas this light chain was localized to respiratory cilia in PCD patient OP-26II1. It is possible that a minor reduction in p28 levels is simply not detected by the resolution offered by IF. Alternatively, the mutation in OP-26II1 occurs in the C-terminus of the protein and it is possible that a truncated CCDC164 protein is made in this patient, resulting in a less severe assembly defect. We were unable to confirm this possibility since CCDC164 antibodies that are useful for IF are not available.

We obtained DNA from the two families (OP-59; OP-39) and found identical homozygous nonsense mutations (Supplementary Fig. 3b) predicting early termination of translation (p.Gln118*) in all three reported PCD individuals. The mutations co-segregated with the disease status consistent with autosomal recessive inheritance of a common founder mutation (Supplementary Fig. 3b). OP-59II1 and II2 are 17-year and 19-year old male siblings. Both have had repeated upper and lower respiratory tract infections since birth. OP-59II1 was operated on by one of the authors (SL) at 6 years of age with mastoidectomy and myringoplasty due to chronic otitis media with therapy-resistant discharge from the ear. There are no other siblings in family OP-59. OP-39II1 is a 32-year old woman having repeated upper and lower respiratory tract infections since infancy. She has been operated on several times for chronic rhinosinusitis and also with pulmonary lobectomy for atelectasis as a child. She has one healthy sibling. In summary, all affected PCD individuals with recessive *CCDC164* mutations display typical symptoms of PCD. Interestingly, none of the four affected individuals had *situs inversus*. We performed whole mount *in situ* hybridization on mouse embryos at embryonic day E7.5 and identified specific expression of *Ccdc164* in the pit cells of the mouse node which carry motile cilia and are also involved in left-right axis development (Supplementary Fig. 8). Therefore, it is not excluded that *CCDC164* mutations also cause randomization of left/right body asymmetry in humans.

Our genetic and ultrastructural findings indicate that a *CCDC164* deficiency in humans disrupts assembly of the N-DRC and resemble the results obtained in *Chlamydomonas* (Fig. 2). To further corroborate our results, we analyzed respiratory cilia for presence of the DRC proteins GAS11 (human DRC4) and LRRC48 (human DRC3). As expected, the *bona fide* DRC proteins GAS11 and LRRC48 were either absent or severely reduced from the ciliary axonemes in all analyzed PCD patients carrying *CCDC164* mutations (Fig. 4), confirming that the *CCD164* deficiency disrupts N-DRC assembly. Previous cryo-electron tomography studies to reconstruct the three-dimensional structure of IDAs as well as the N-DRC in *Chlamydomonas pf3* mutants[13,28] are consistent with our observations in *CCDC164*-mutant cilia. The *pf3* mutant lacks large parts of the N-DRC structure and has reduced levels of several DRC subunits[7,8,9,13,14].

CCDC164 mutations result in defective N-DRC assembly and ciliary movement

Recently, we, and others, found that recessive mutations in *CCDC39* and *CCDC40* cause PCD with severe ultrastructural defects such as marked tubular disorganization with

displacement of peripheral outer doublets as well as the central pair apparatus and associated IDA defects[10,11,29]. Defective N-DRC and inner dynein arm assembly in *CCDC39* and *CCDC40* mutant cilia is characterized by absence of the DRC component GAS11 (DRC4) and the inner dynein arm light chain DNALI1 (orthologous to *Chlamydomonas* light chain p28) from the ciliary axonemes. In addition, human *CCDC39* / *CCDC40* mutant cilia lack axonemal CCDC39 localization. Therefore, we examined CCDC39 and DNALI1 localization in *CCDC164* mutant respiratory cells. In contrast to PCD patients with *CCDC39* and *CCDC40* mutations and to our results in *Chlamydomonas* with the *pf3* mutant, the axonemal localization of the IDA protein DNALI1 was not altered in any of the four PCD patients carrying *CCDC164* mutations (Supplementary Fig. 7). Consistently, we found normal axonemal CCDC39 localization in *CCDC164* mutant respiratory cilia (Supplementary Fig. 7), indicating that assembly of CCDC39 is not dependent on CCDC164/DRC1 function, which is also consistent with the results observed in *pf3* axonemes from *Chlamydomonas* (Fig. 2d).

Thus, we provide genetic evidence that defects in the human *CCDC164/DRC1* gene result in a novel PCD variant characterized by defects of the N-DRC links. Given the clinical manifestations of PCD and the phenotype of the *Chlamydomonas pf3* mutant, we predicted that *CCDC164*-defective respiratory cilia would display abnormal cilia beating (a combination of ciliary beat frequency and ciliary waveform). To examine the functional consequences directly, we performed high-speed video microscopy of vital nasal ciliated respiratory cells obtained by nasal brush biopsies from normal individuals and the OP-26II1 patient[30]. Respiratory cilia from the OP-26II1 showed an increased beat frequency (12 Hz at room temperature vs. 4–8 Hz for controls), a finding not observed in *Chlamydomonas pf3* mutants where flagellar beat frequencies are equal to slightly reduced compared to wild type[15]. While the waveform patterns of *Chlamydomonas* flagella and human cilia are distinct, both show the characteristic decreased amplitude of bending associated with defects in the N-DRC (Supplementary movies 1–4, Fig. 5[15]).

The degree of reduction of the beating amplitude is less severe than that observed in *CCDC39* and *CCDC40* mutant respiratory cilia, where we previously demonstrated a combined defect of N-DRC and inner dynein arm assembly[10,11]. These differences in motility indicate that CCDC39/CCDC40 mutations may have a more severe defect on N-DRC and/or inner dynein arm assembly or function. Computer image averaging of CCDC39 mutant axonemes in thin section have recently demonstrated structural defects that extend beyond the N-DRC region[12]. Thus, CCDC39/CCDC40 may be part of an unidentified N-DRC density and serve as a N-DRC docking domain or associate with a closely connected axoneme sub-structure[13].

Discussion

Taken together, our findings provide strong evidence for the role of DRC1 in ciliary function and identify *CCDC164* mutations as a cause for an autosomal recessive variant of PCD. Based on our data, we propose that DRC1 is a highly conserved structural component of the N-DRC, which is essential for N-DRC integrity. In addition, it functions in the assembly and regulation of specific classes of inner dynein arm motors and may also function to restrict dynein-driven microtubule sliding, thus aiding in the generation of ciliary bending[7,8,9,13,14]. We strongly believe that this particular type of PCD variant can be easily overlooked by conventional TEM unless careful ultrastructural analyses of the micrographs and high-speed video microscopy to assess ciliary waveform are performed. Therefore, the diagnosis of this PCD variant is greatly aided by the demonstration of axonemal GAS11 and LRRC48 reduction by high-resolution immunofluorescence microscopy. Similar to findings for the outer dynein arm[31], the identification and molecular characterization of DRC1 and

other N-DRC components will greatly aid the ongoing and future diagnosis of PCD. In addition, *Chlamydomonas* will continue to reveal conserved genes important for ciliary assembly and movement that when defective, result in PCD.

Online Methods

Identification, mapping and molecular analyses of *DRC1*

DRC1 peptides, identified using direct amino acid sequencing of partially purified DRC1 protein (Gianni Piperno, Mount Sinai School of Medicine) were used to identify *DRC1* sequences in the *Chlamydomonas* genome database. *Chlamydomonas* genomic sequences (TIN310364.b1) were used to identify overlapping *Volvox* genomic sequences (ABSY90570.g1, ABSY145737.g1, ABSY130275.g1, ABSY97608.g1, ABSY146505.g1, ABSY227857.b1), which were then used to blast NCBI to identify a Human DRC1 ortholog (NP_659475.2). Analysis of the *Chlamydomonas* Genome Database with NP_659475.2 revealed additional *Chlamydomonas* genomic sequences in the 5′ and 3′ end of the *DRC1* gene. The full-length *Chlamydomonas DRC1* cDNA was cloned using a combination of PCR and RT-PCR methods and analysis of version 3 of the *Chlamydomonas* genome database, which has some *DRC1* sequences assigned to scaffolds 340, 221, and 2717 (Supplementary Fig. 1a, Supplementary Table 2). Additional primers were designed based on homology to a closely related sequence in the *Volvox* genome. Linkage analyses and molecular methods were performed as described[17,34]. To order the molecular map and identify sequences linked to the *pf3* mutation, a *pf3 mt+* strain was crossed to the polymorphic strain *S1–D2, mt−*, and the progeny of 30 tetrads were analyzed for sequence polymorphisms. Molecular markers were tested for *pf3* linkage (Supplementary Figs. 1d and e) and are listed in Supplementary Table 3. The *VFL1* gene is located within 60 kb of both HSP70 and GP337 and anchors the molecular map on the right arm of Linkage Group VIII[34], whereas linkage to *pf3* anchors the molecular map to the left arm of Linkage Group VIII (Supplementary Fig. 1e). Methods for the isolation of genomic DNA, RNA, Southern and Northern blotting, PCR, and RT-PCR are described in detail[17,34]. The *CRY1* gene encoding ribosomal protein S14, used as a loading control for Northern blots, is described[50].

Cell culture, flagellar isolation and fractionation

Chlamydomonas strains are listed in Supplementary Table 4. Cell culture, genetic analyses and flagellar isolations were performed as described[51,52], except flagella were demembranated with IGEPAL CA-630 (Sigma Aldrich, St. Louis, MO). Isolated axonemes were sequentially extracted with 0.6M NaCl and 0.2–0.6M NaI to generate NaCl and NaI extracts and extracted outer doublet microtubules. All fractions were separated by SDS-PAGE and analyzed by immunoblot using antibodies as described in Supplementary Table 5. Velocity sedimentation on sucrose density gradients were performed as described[53].

Production of a DRC1 specific antibody

A region of the DRC1 cDNA encoding amino acids 155–243 was PCR amplified and subcloned into the pCR2.1 TOPO cloning vector to generate plasmid pMW199.1. The insert from pMW199.1 was excised using *Eco*R1 and subcloned into the *Eco*R1 site of pET28A to generate plasmid pMW219.15, which was sequenced to confirm orientation. The resulting His-tagged DRC1 fusion protein was expressed, purified over a Nickel column (EMD Chemicals, Gibbstown, NJ) and used as an antigen to immunize two rabbits (Spring Valley Labs, Woodbine, MD). A DRC1-MBP fusion was created by excising the insert from pMW1991 with *Eco*R1 and subcloning into the *Eco*R1 site of pMal-C (New England Biolabs) to produce plasmid pMW260.1. The resulting antisera were either used directly, blot affinity purified against the DRC1-MBP fusion protein, or column affinity purified using the DRC1-MBP fusion protein coupled to agarose resin (New England Biolabs,

Cambridge, MA USA). Some batches of antibody were also purified by pre-absorption with methanol fixed *pf3* cells.

Mass Spectral Counting

Wild-type and *pf3* DHC content were analyzed by mass spectrometry at the Center for Mass Spectrometry and Proteomics. For each DHC identified, we noted both the number of unique peptides and the total number of assigned spectra. The total number of spectra for each inner arm DHC was normalized to the total number of spectra for the I1 DHC subunits (which are not affected by the *pf3* mutation[13,14], Fig. 2d). The numbers for each inner arm DHC are calculated as a fraction of the total I1 DHCs, converted to percentage and then plotted on a graph.

PCD Patients and families

Signed and informed consent was obtained from individuals fulfilling the diagnostic criteria of PCD and their family members using protocols approved by the Institutional Ethics Review Board at the University of Freiburg and Muenster and collaborating institutions[54]. Genomic DNA was isolated via standard methods from blood samples or from lymphocyte cultures after Epstein-Barr virus transformation. We analyzed 20 unrelated PCD families with defects involving the N-DRC for the presence of mutations in the *CCDC164* gene.

Imaging of human respiratory cilia

Ultrastructural and immunofluorescence analyses of human respiratory cilia from nasal brush biopsies were performed as described[10]. Ciliary beating was assessed using video microscopy as described[10].

In situ hybridization

Sense and antisense probes were generated using digoxigenin NTPs (Roche) and T7 or SP6 RNA polymerases, respectively. Whole mount *in situ* hybridization was performed according to standard procedures with minor modifications[55]. Images were captured using a Scion CFW-1310C camera mounted on an Axioskop 2 plus microscope (Zeiss) and Image-Pro Express.

Supplementary Material

Refer to Web version on PubMed Central for supplementary material.

Acknowledgments

The authors wish to thank Gianni Piperno for providing the peptide sequences used to identify the *Chlamydomonas DRC1* gene. MEP also thanks Catherine Perrone, Thuc vy Le, Andrew Bostrom, Joshua Mueller, and Julie Ann Knott (University of Minnesota (UMN)) for assistance with mapping the *DRC1 l*ocus, Pushpa Kathir (UMN), Carolyn Silflow (UMN), and Susan Dutcher (Washington University) for advice on RFLP mapping, and Todd Markowski and Bruce Witthun of the Center for Computational Proteomics at the UMN for assistance with mass spectrometry and spectral counting. We also thank Angelina Heer (University of Freiburg) and Cordula Westermann (University Hospital Muenster) for excellent technical assistance. We thank Matt Laudon and the *Chlamydomonas* Genetics Center for strains. For antibodies we thank Richard Linck (University of Minnesota), Mark Sanders (University of Minnesota), Ritsu Kamiya (University of Tokyo), Toshiki Yagi (Kyoto University), Pinfen Yang (Marquette University), Elizabeth Smith (Dartmouth University), and Gianni Piperno (Mount Sinai School of Medicine). This work was supported by NIH grants to MEP (GM-55667) and WSS (GM-051173), an NRSA postdoctoral fellowship to MW (GM-075446), funding to WSS from the Children's Healthcare of Atlanta and Emory University School of Medicine Pediatric Research Center and funding to Heymut Omran (the "Deutsche Forschungsgemeinschaft" DFG Om 6/4, GRK1104, SFB592, IZKF Muenster and the CEDAD graduate school as well as SYSCILIA from the European community). The Center for Mass Spectrometry and Proteomics at the University of Minnesota is supported by multiple grants including NSF Major Research Instrumentation grants

9871237 and NSF-DBI-0215759. Technical and software support was also provided by the Minnesota Supercomputing Institutute.

References

1. Fliegauf M, Benzing T, Omran H. When cilia go bad: cilia defects and ciliopathies. Nat Rev Mol Cell Biol. 2007; 8:880–893. [PubMed: 17955020]
2. Zariwala MA, Omran H, Ferkol TW. The emerging genetics of primary ciliary dyskinesia. Proc Am Thorac Soc. 2011; 8:430–433. [PubMed: 21926394]
3. Mazor M, et al. Primary ciliary dyskinesia caused by homozygous mutation in DNAL1, encoding dynein light chain 1. Am J Hum Genet. 2011; 88:599–607. [PubMed: 21496787]
4. Olbrich H, et al. Mutations in DNAH5 cause primary ciliary dyskinesia and randomization of left-right asymmetry. Nat Genet. 2002; 30:143–144. [PubMed: 11788826]
5. Panizzi JR, et al. CCDC103 mutations cause primary ciliary dyskinesia by disrupting assembly of ciliary dynein arms. Nat Genet. 2012; 44:714–719. [PubMed: 22581229]
6. Smith EF, Yang P. The radial spokes and central apparatus: mechano-chemical transducers that regulate flagellar motility. Cell Motil Cytoskeleton. 2004; 57:8–17. [PubMed: 14648553]
7. Huang B, Ramanis Z, Luck DJ. Suppressor mutations in *Chlamydomonas* reveal a regulatory mechanism for flagellar function. Cell. 1982; 28:115–124. [PubMed: 6461414]
8. Piperno G, Mead K, LeDizet M, Moscatelli A. Mutations in the “dynein regulatory complex” alter the ATP-insensitive binding sites for inner arm dyneins in *Chlamydomonas* axonemes. J Cell Biol. 1994; 125:1109–1117. [PubMed: 8195292]
9. Piperno G, Mead K, Shestak W. The inner dynein arms I2 interact with a “dynein regulatory complex” in *Chlamydomonas* flagella. J Cell Biol. 1992; 118:1455–1463. [PubMed: 1387875]
10. Becker-Heck A, et al. The coiled-coil domain containing protein CCDC40 is essential for motile cilia function and left-right axis formation. Nat Genet. 2010; 43:79–84. [PubMed: 21131974]
11. Merveille AC, et al. CCDC39 is required for assembly of inner dynein arms and the dynein regulatory complex and for normal ciliary motility in humans and dogs. Nat Genet. 2010; 43:72–78. [PubMed: 21131972]
12. O’Toole ET, Giddings TH Jr, Porter ME, Ostrowski LE. Computer-assisted image analysis of human cilia and *Chlamydomonas* flagella reveals both similarities and differences in axoneme structure. Cytoskeleton (Hoboken). 2012; 69:577–90. [PubMed: 22573610]
13. Heuser T, Raytchev M, Krell J, Porter ME, Nicastro D. The dynein regulatory complex is the nexin link and a major regulatory node in cilia and flagella. J Cell Biol. 2009; 187:921–933. [PubMed: 20008568]
14. Gardner LC, O’Toole E, Perrone CA, Giddings T, Porter ME. Components of a “dynein regulatory complex” are located at the junction between the radial spokes and the dynein arms in *Chlamydomonas* flagella. J Cell Biol. 1994; 127:1311–1325. [PubMed: 7962092]
15. Brokaw CJ, Kamiya R. Bending patterns of *Chlamydomonas* flagella: IV. Mutants with defects in inner and outer dynein arms indicate differences in dynein arm function. Cell Motil Cytoskeleton. 1987; 8:68–75. [PubMed: 2958145]
16. Kabututu ZP, Thayer M, Melehani JH, Hill KL. CMF70 is a subunit of the dynein regulatory complex. J Cell Sci. 2010; 123:3587–3595. [PubMed: 20876659]
17. Rupp G, Porter ME. A subunit of the dynein regulatory complex in *Chlamydomonas* is a homologue of a growth arrest-specific gene product. J Cell Biol. 2003; 162:47–57. [PubMed: 12847082]
18. Colantonio JR, et al. The dynein regulatory complex is required for ciliary motility and otolith biogenesis in the inner ear. Nature. 2009; 457:205–209. [PubMed: 19043402]
19. Lin J, et al. Building blocks of the nexin-dynein regulatory complex in *Chlamydomonas* flagella. J Biol Chem. 2011; 286:29175–29191. [PubMed: 21700706]
20. Silflow CD, et al. Expression of flagellar protein genes during flagellar regeneration in *Chlamydomonas*. Cold Spring Harb Symp Quant Biol. 1982; 46(Pt 1):157–169. [PubMed: 6179692]

21. Dymek EE, Heuser T, Nicastro D, Smith EF. The CSC is required for complete radial spoke assembly and wild-type ciliary motility. Mol Biol Cell. 2011; 22:2520–2531. [PubMed: 21613541]
22. Yanagisawa HA, Kamiya R. A tektin homologue is decreased in *Chlamydomonas* mutants lacking an axonemal inner-arm dynein. Mol Biol Cell. 2004; 15:2105–2115. [PubMed: 14978211]
23. Yagi T, Uematsu K, Liu Z, Kamiya R. Identification of dyneins that localize exclusively to the proximal portion of *Chlamydomonas* flagella. J Cell Sci. 2009; 122:1306–1314. [PubMed: 19351714]
24. Bui KH, Yagi T, Yamamoto R, Kamiya R, Ishikawa T. Polarity and asymmetry in the arrangement of dynein and related structures in the *Chlamydomonas* axoneme. J Cell Biol. 2012; 198:913–924. [PubMed: 22945936]
25. Zadro C, et al. Five new OTOF gene mutations and auditory neuropathy. Int J Pediatr Otorhinolaryngol. 2010; 74:494–498. [PubMed: 20211493]
26. Mateos-Corral D, Coombs R, Grasemann H, Ratjen F, Dell SD. Diagnostic value of nasal nitric oxide measured with non-velum closure techniques for children with primary ciliary dyskinesia. J Pediatr. 2011; 159:420–424. [PubMed: 21514598]
27. Carlén B, Lindberg S, Stenram U. Absence of nexin links as a possible cause of primary ciliary dyskinesia. Ultrastruct Pathol. 2003; 27:123–126. [PubMed: 12746204]
28. Bui KH, Sakakibara H, Movassagh T, Oiwa K, Ishikawa T. Molecular architecture of inner dynein arms in situ in *Chlamydomonas reinhardtii* flagella. J Cell Biol. 2008; 183:923–932. [PubMed: 19029338]
29. Blanchon S, et al. Delineation of CCDC39/CCDC40 mutation spectrum and associated phenotypes in primary ciliary dyskinesia. J Med Genet. 2012; 49:410–6. [PubMed: 22693285]
30. Fliegauf M, et al. Mislocalization of DNAH5 and DNAH9 in respiratory cells from patients with primary ciliary dyskinesia. Am J Respir Crit Care Med. 2005; 171:1343–1349. [PubMed: 15750039]
31. Pazour GJ, Agrin N, Walker BL, Witman GB. Identification of predicted human outer dynein arm genes: candidates for primary ciliary dyskinesia genes. J Med Genet. 2006; 43:62–73. [PubMed: 15937072]
32. Yang P, Sale WS. The Mr 140,000 intermediate chain of *Chlamydomonas* flagellar inner arm dynein is a WD-repeat protein implicated in dynein arm anchoring. Mol Biol Cell. 1998; 9:3335–3349. [PubMed: 9843573]
33. Heuser T, Dymek EE, Lin J, Smith EF, Nicastro D. The CSC connects three major axonemal complexes involved in dynein regulation. Mol Biol Cell. 2012; 23:3143–3155. [PubMed: 22740634]
34. Kathir P, et al. Molecular map of the *Chlamydomonas reinhardtii* nuclear genome. Eukaryot Cell. 2003; 2:362–379. [PubMed: 12684385]
35. Proschold T, Harris EH, Coleman AW. Portrait of a species: *Chlamydomonas reinhardtii*. Genetics. 2005; 170:1601–1610. [PubMed: 15956662]
36. Gross CH, Ranum LP, Lefebvre PA. Extensive restriction fragment length polymorphisms in a new isolate of *Chlamydomonas reinhardtii*. Curr Genet. 1988; 13:503–508. [PubMed: 2900078]
37. Mitchell DR, Rosenbaum JL. A motile *Chlamydomonas* flagellar mutant that lacks outer dynein arms. J Cell Biol. 1985; 100:1228–1234. [PubMed: 3156867]
38. Rupp G, O'Toole E, Gardner LC, Mitchell BF, Porter ME. The *sup-pf-2* mutations of *Chlamydomonas* alter the activity of the outer dynein arms by modification of the gamma-dynein heavy chain. J Cell Biol. 1996; 135:1853–1865. [PubMed: 8991096]
39. Porter ME, Power J, Dutcher SK. Extragenic suppressors of paralyzed flagellar mutations in *Chlamydomonas reinhardtii* identify loci that alter the inner dynein arms. J Cell Biol. 1992; 118:1163–1176. [PubMed: 1387404]
40. LeDizet M, Piperno G. *ida4-1*, *ida4-2*, and *ida4-3* are intron splicing mutations affecting the locus encoding p28, a light chain of *Chlamydomonas* axonemal inner dynein arms. Mol Biol Cell. 1995; 6:713–723. [PubMed: 7579690]

41. Ikeda K, et al. Rib72, a conserved protein associated with the ribbon compartment of flagellar A-microtubules and potentially involved in the linkage between outer doublet microtubules. J Biol Chem. 2003; 278:7725–7734. [PubMed: 12435737]
42. Yamamoto R, Yanagisawa HA, Yagi T, Kamiya R. Novel 44-kilodalton subunit of axonemal dynein conserved from *Chlamydomonas* to mammals. Eukaryot Cell. 2008; 7:154–161. [PubMed: 17981992]
43. Yamamoto R, Yanagisawa HA, Yagi T, Kamiya R. A novel subunit of axonemal dynein conserved among lower and higher eukaryotes. FEBS Lett. 2006; 580:6357–6360. [PubMed: 17094970]
44. Yang C, Compton MM, Yang P. Dimeric novel HSP40 is incorporated into the radial spoke complex during the assembly process in flagella. Mol Biol Cell. 2005; 16:637–648. [PubMed: 15563613]
45. Dymek EE, Smith EF. A conserved CaM- and radial spoke associated complex mediates regulation of flagellar dynein activity. J Cell Biol. 2007; 179:515–526. [PubMed: 17967944]
46. Salisbury JL, Baron AT, Sanders MA. The centrin-based cytoskeleton of *Chlamydomonas reinhardtii*: distribution in interphase and mitotic cells. J Cell Biol. 1988; 107:635–641. [PubMed: 3047144]
47. LeDizet M, Piperno G. The light chain p28 associates with a subset of inner dynein arm heavy chains in *Chlamydomonas* axonemes. Mol Biol Cell. 1995; 6:697–711. [PubMed: 7579689]
48. Rashid S, et al. The *murine Dnali1* gene encodes a flagellar protein that interacts with the cytoplasmic dynein heavy chain 1. Mol Reprod Dev. 2006; 73:784–794. [PubMed: 16496424]
49. Colantonio JR, et al. Expanding the role of the dynein regulatory complex to non-axonemal functions: association of GAS11 with the Golgi apparatus. Traffic. 2006; 7:538–548. [PubMed: 16643277]
50. Nelson JA, Savereide PB, Lefebvre PA. The *CRY1* gene in *Chlamydomonas reinhardtii*: structure and use as a dominant selectable marker for nuclear transformation. Mol Cell Biol. 1994; 14:4011–4019. [PubMed: 8196640]
51. Harris, E. The Chlamydomonas Sourcebook. Harris, E., editor. Vol. 1. Academic Press; 2009. p. 241-301.Ch. 8
52. Witman GB. Isolation of *Chlamydomonas* flagella and flagellar axonemes. Methods Enzymol. 1986; 134:280–290. [PubMed: 3821567]
53. Bower R, et al. IC138 defines a subdomain at the base of the I1 dynein that regulates microtubule sliding and flagellar motility. Mol Biol Cell. 2009; 20:3055–3063. [PubMed: 19420135]
54. Barbato A, et al. Primary ciliary dyskinesia: a consensus statement on diagnostic and treatment approaches in children. Eur Respir J. 2009; 34:1264–1276. [PubMed: 19948909]
55. Thisse C, Thisse B. High-resolution *in situ* hybridization to whole-mount zebrafish embryos. Nature protocols. 2008; 3:59–69.

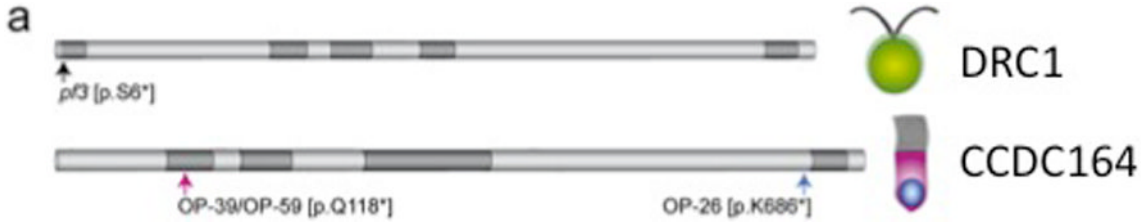

Figure 1. Localisation of mutations within *Chlamydomonas* and humans

Diagram of the DRC1 subunit in *Chlamydomonas* (top) and its human orthologue CCDC164 (bottom). The coiled coil motifs are drawn in dark grey, the positions of the mutations identified in algae and human are indicated with arrows.

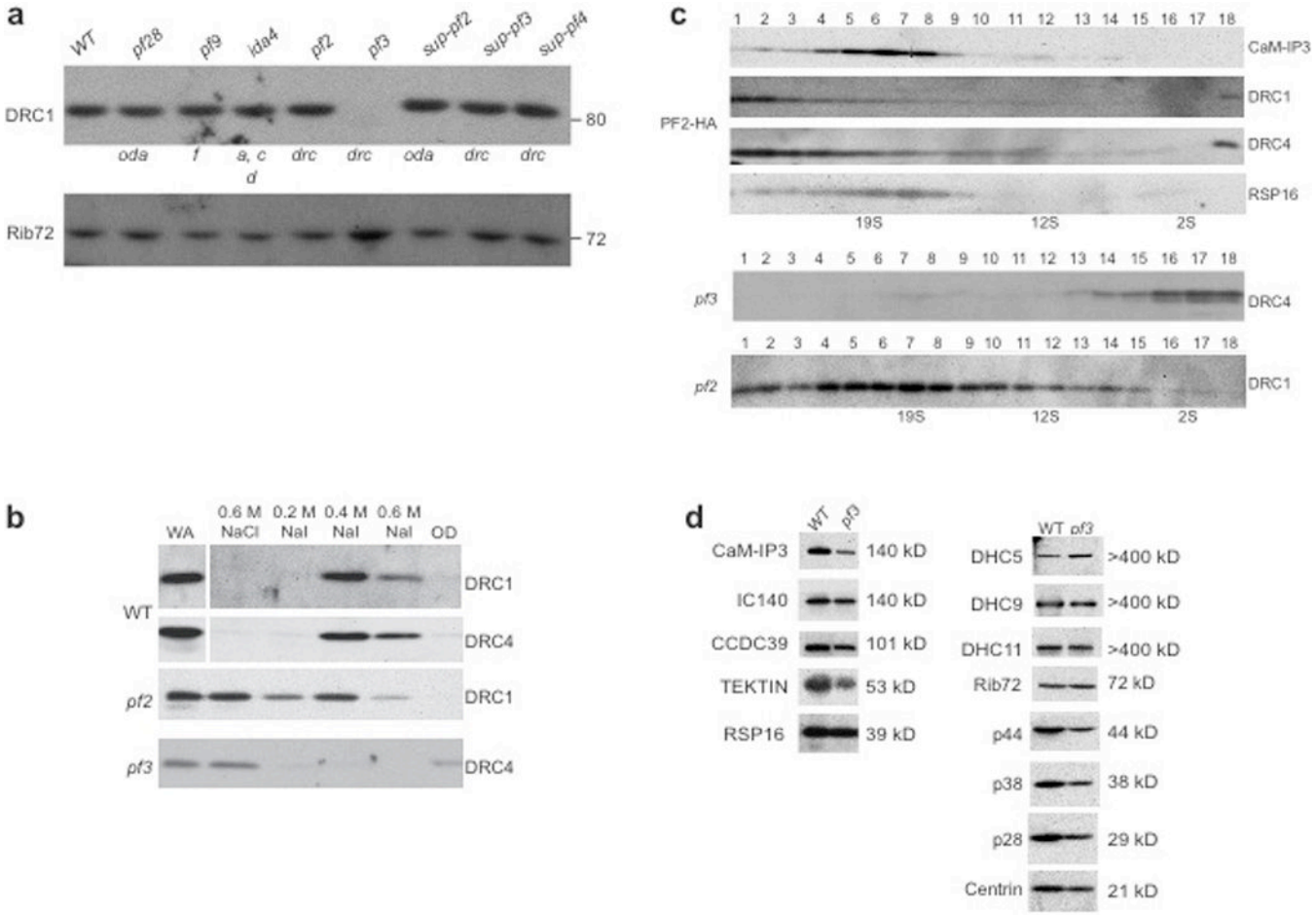

Figure 2. The *Chlamydomonas pf3* mutant is defective in DRC1 resulting in disruption of N-DRC integrity

(**a**) Western blot analysis of WT and *Chlamydomonas* mutant axonemes defective in the outer arm (*pf28*, *sup-pf-2*), inner arms (*pf9*, *ida4*) and N-DRC (*pf2* (*DRC4*), *pf3* (*DRC1*), *sup-pf-3*, *sup-pf-4* (*DRC5*)) reveal that DRC1 is specifically missing in the *drc*- mutant *pf3*. Note, longer exposures of *pf3* mutant axonemes reveals a very faint band that is missing in wild-type (not shown) suggesting that re-initiation of translation at a downstream methionine may occur at very low levels in the *pf3* mutant. (**b**) Analysis of ciliary extracts reveal that DRC1 is extracted from the axoneme using 0.4–0.6 M NaI in WT, along with other DRC subunits (DRC4 shown). In the *drc* mutants, *pf2* and *pf3*, the residual N-DRC structure is extracted more readily as shown by its release from the axoneme using high salt buffers (0.6 M NaCl) or lower molarity NaI buffers (0.2 M NaI). (**c**) Velocity sedimentation of NaI extracts from wild-type (PF2-HA) on sucrose density gradients reveal that the N-DRC (DRC1 and DRC4) sediments as a very large complex (>19S). Sedimentation of RSP16 of the radial spokes is shown as a control. In contrast, in the *drc*- mutants, *pf2* and *pf3*, the residual N-DRC structure remaining in these mutant axonemes is readily disrupted. DRC1 sediments at ~19S in *pf2*, and DRC4 sediments at ~2S in *pf3*. (**d**) The *drc1* mutation in *pf3* results in altered levels of inner arm components (p44, p38, p28, and centrin), tektin and the CSC (CaM-IP3). Antibodies to DHC5, DHC9 and DHC11 suggest that these inner arm heavy chains are not significantly reduced in the *pf3* mutant. There are no observable defects in the levels of the radial spokes (RSP16), dynein *f* (IC140), CCDC39 or Rib72.

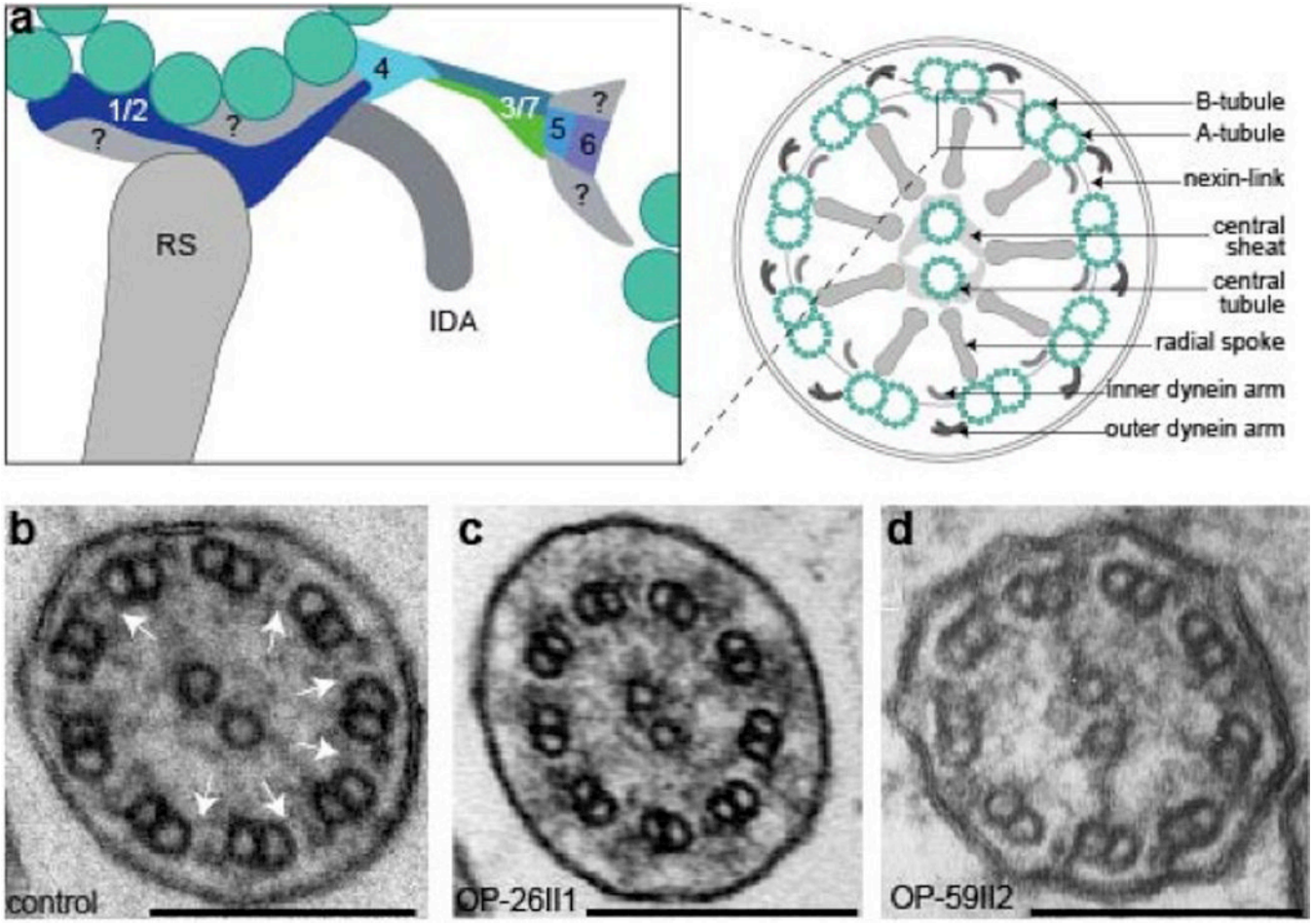

Figure 3. Mutations in the *CCDC164* gene in humans result in defects in the N-DRC links

(**a**) Schematic diagram of the 9+2 cilium and the N-DRC structure (modified after Lin et al. 2011) enlarged to show the predicted locations of N-DRC subunits. Transmission electron microscopy of respiratory cilia shows normal axonemal structure in the control (**b**) and normal tubular organization in *CCDC164*-mutant cilia (**c, d**). N-DRC links connecting outer doublets are depicted with arrows in the control (**b**). In patients OP-26II1 and OP-59II2 with homozygous nonsense *CCDC164* mutations (**c, d**) the N-DRC links are missing (N = 12). Black scale bars (a–c) represent 0.2μm.

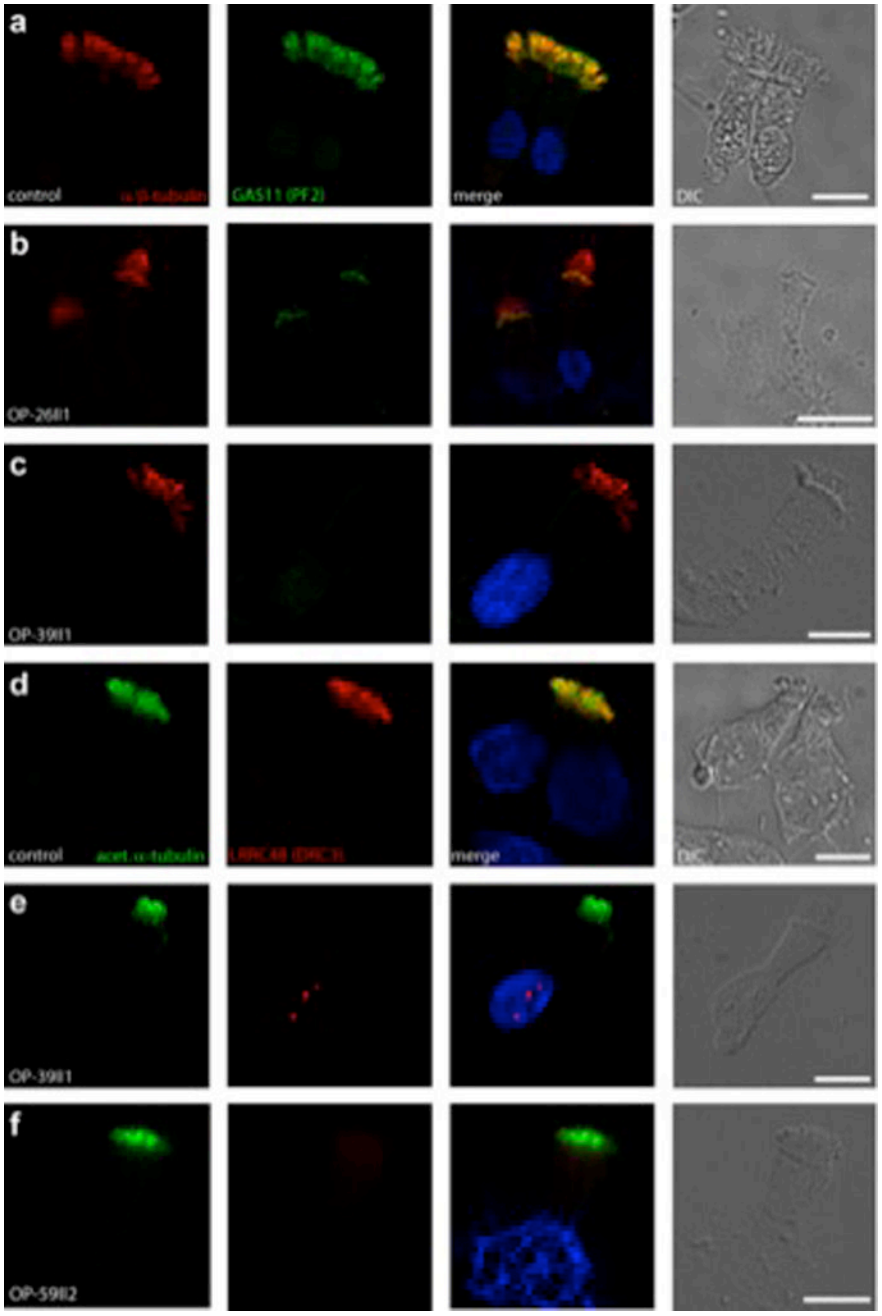

Figure 4. The *CCDC164*- mutations result in defective N-DRC assembly in respiratory cilia

High-resolution immuno-fluorescence analysis of the subcellular localization of GAS11 (DRC4) and LRRC48 (DRC3) in respiratory cells from controls (**a** and **d**) and PCD patients OP-26II1 (**b**), OP-39II1 (**c** and **e**) and OP-59II2 (**f**) carrying mutations in the *CCDC164* gene. Axoneme-specific antibodies against α/β-tubulin (red, **a**, **b** and **c**) and acetylated α-tubulin (green, **d**, **e** and **f**) were used as axonemal control. Nuclei were stained with Hoechst 33342 (blue). In respiratory epithelial cells from controls, GAS11 (green, **a**) and LRRC48 (red, **d**) localize to the entire length of the axonemes. In respiratory epithelial cells from the patients carrying *CCDC164*-mutations, GAS11 (shown for patients OP-26II1 (**b**) and OP-39II1 (**c**) and LRRC48 (shown for patients OP-39II1 (**e**) and OP-59II2 (**f**) were completely absent from the ciliary axonemes. The yellow co-staining within the ciliary

axoneme (**a** and **d**) indicates that both proteins co-localize within respiratory cilia. White scale bars indicate 10μm.

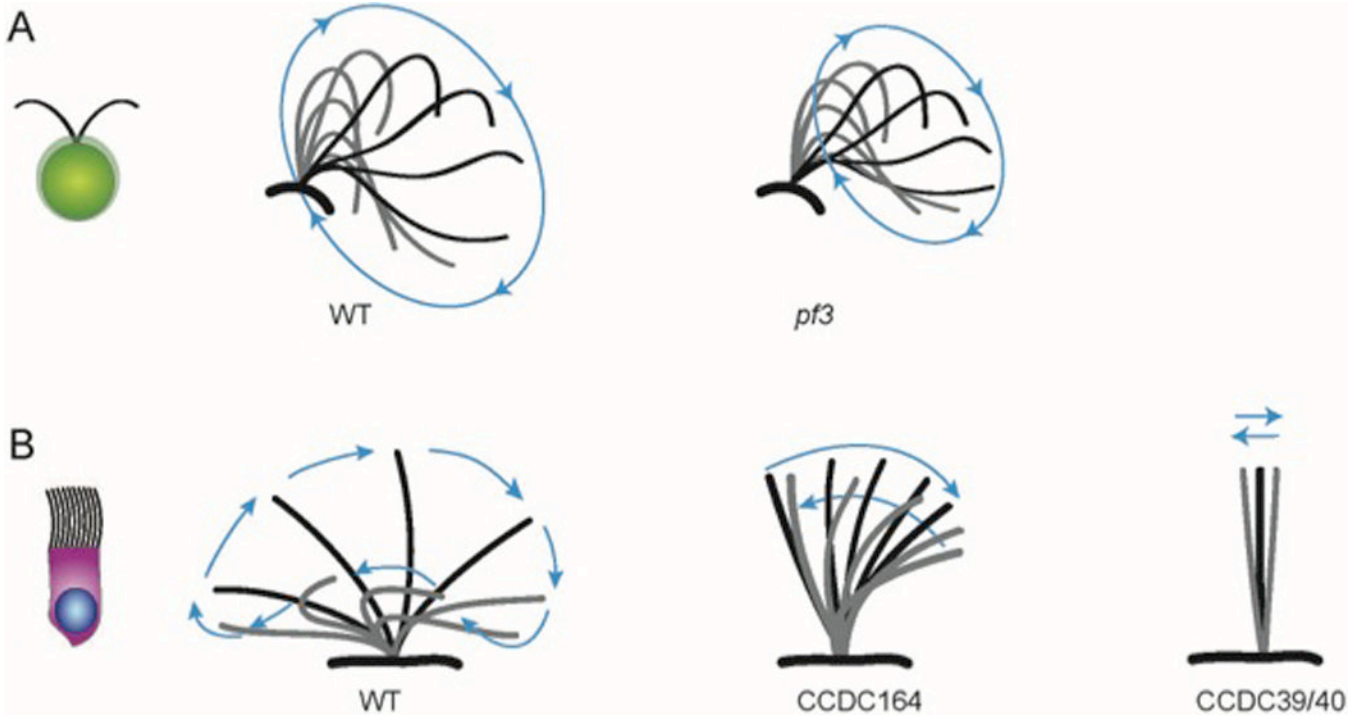

Figure 5. Comparison of axonemal bending patterns in *Chlamydomonas* and human respiratory cilia

(**a**) The beating pattern of *pf3* mutant cilia (defective in *DRC1*) exhibits reduced amplitude and bending. (**b**) Respiratory cilia from individuals with mutations in the *CCDC164* gene (orthologue of *DRC1*) are also reduced in the amplitude (grey) and appear stiff when compared to wild type. *CCDC164* mutant cilia show a less severe phenotype compared to *CCDC39* or *CCDC40* mutants, which are characterized by strongly reduced amplitude and stiff and rigid cilia. (Black = effective stroke, Grey = recovery stroke). Illustrations in (**a**) are adapted and modified from Brokaw and Kamiya, 1987[15].